MEASURING THE PARAMETERS OF A DISPERSED-ANNULAR FLOW

M. V. Davydova, V. N. Zelenskii,
and P. L. Kirillov

UDC 541.182.2

We present certain experimental data on the parameters of the dispersed-annular flow of a vapor–water mixture; these data have been derived with a tube 18 mm in diameter, 3 m in length, and for the following range of variations in the basic parameters: the weight velocities varied from 145 to 400 kg/m^2·sec; the pressures varied from 9.8 to 49 N/cm^2; and finally, the vapor content varied from 0 to 0.5. We derived results on film thickness, the boundaries of existence for a dispersed-annular flow regime, the pressure gradient, and the volumetric vapor content.

In terms of structure, a dispersed-annular flow represents the flow – through the central portion of a tube – of a gas or vapor phase containing liquid droplets, together with an annular liquid film moving along the wall. We have an exchange of heat between these two regions, in addition to the transfer of momentum and mass.

The unique features of the hydrodynamic and heat transfer which are manifested in the dispersed-annular flow of a two-phase mixture are associated to a considerable extent with the phase distribution over the cross section of the vapor-generating channel. The theoretical solutions proposed in recent years are based on hypotheses which cannot presently be proved. In this connection, the derivation of experimental results is extremely important.

We studied the boundaries for the existence of a dispersed-annular flow regime on a low-pressure test stand; we measured the thickness of the liquid film, the true volumetric vapor content in the region at the wall, and also the length of the hydrodynamic-stabilization segment, this quantity being determined from the thickness of the liquid film. All of the tests were conducted with a vapor–water mixture.

The test section consisted of a stainless-steel tube with a 22 × 2 diameter and a length of 3000 mm. The heating of the liquid and that of the working section were accomplished by passing an alternating current from OSU-80 transformers through the tube. The power was regulated by means of AOMK autotransformers. The heater made it possible to supply the working section with heated water or with a heated mixture exhibiting a specified vapor content by weight. The length of the heated section could be altered by moving

TABLE 1. Results from the Measurement of the Boundaries of Existence for a Dispersed-Annular Flow Regime

l, m	G, kg/h	l_1, m	x_{in}	x_1	x_b	$q\cdot10^{-6}$, kcal/m^3·h
2,0	228	1,0	–0,110	0,040	0,198	0,322
2,0	300	1,0	–0,110	0,030	0,161	0,383
2,0	480	1,0	–0,150	0,035	0,176	0,702
4,0	484	1,5	0,095	0,033	0,329	0,479
4,0	568	2,1	0,026	0,036	0,307	0,662
4,0	626	2,3	0,005	0,038	0,260	0,654
5,0	240	0,75	0,405	0,042	0,416	—
5,0	302	0,92	0,436	0,030	0,448	—
5,0	360	1,2	0,180	0,033	0,500	0,249
5,0	425	1,4	0,143	0,034	0,406	0,326
5,0	478	1,6	0,094	0,034	0,397	0,417

Physics and Power-Engineering Institute, Obninsk. Translated from Inzhenerno-Fizicheskii Zhurnal, Vol. 17, No. 1, pp. 5-12, July, 1969. Original article submitted September 16, 1968.

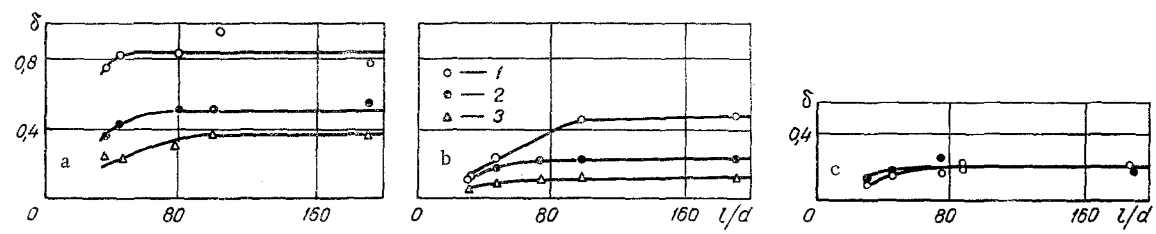

Fig. 1. Length of the stabilization section (mm), determined from the thickness of the film in the dispersed-annular flow (a shows x = 0.03-0.043; b shows x = 0.075-0.108; c shows x = 0.155-0.178) for various gravimetric vapor contents: 1) 370 kg/h; 2) 300 kg/h; 3) 240 kg/h.

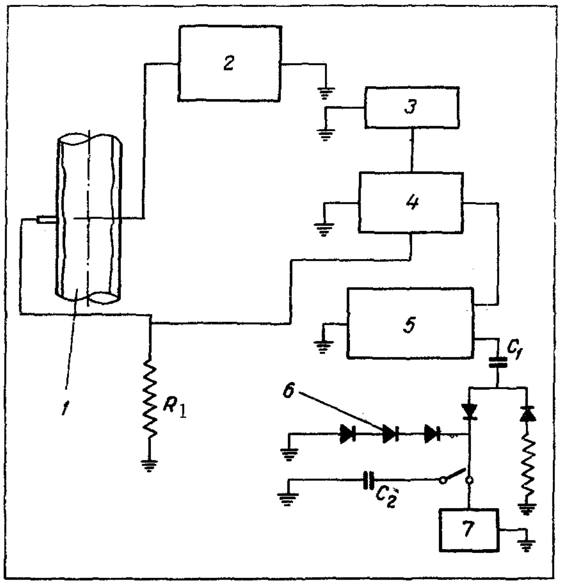

Fig. 2. Circuit for the probe to measure film thickness: 1) experimental section; 2) ZG-11 sound-pulse generator; 3) N-700 loop oscillograph; 4) measuring amplifier; 5) S1-18 oscillograph; 6) limiter diodes; 7) PST-100 counter.

specially designed current conductors. The stand was designed so as to permit changing the experimental section from a free space – when moving the distillate from the condenser to the pump tank – to a flowthrough section – when moving the distillate directly from the condenser to the pump inlet. A constant flow rate within a given regime is maintained by means of manually operated valves installed ahead of the heater and at the outlet from the working section. The parameters varied over the following limits: the flow rate ranged from 140 through 700 kg/h; the pressure at the outlet from the experimental section varied from 1 to 5 atm abs; the gravimetetric vapor content ranged as high as 0.5.

The data in the literature on the transition boundaries between various flow regimes in vapor–liquid mixtures are exceedingly few in number [1-4], and they encompass an inadequate range of variations in the basic parameters. The existing results have been derived primarily from air–water mixtures. In developing the analytical model of the heat-transfer crises in a dispersed-annular flow it became necessary experimentally to determine the boundaries for the regions within which this form of flow could exist. These determinations were accomplished by means of an electric resistance probe connected to an oscillograph whose screen showed the voltage pulses corresponding to the various phases. The boundary of the transition from the dispersed-annular regime to the dispersed regime was determined by setting up the probe at a distance of 0.02-0.03 mm from the tube wall. When the average film thickness reached this magnitude, all further increase in power was stopped to avoid the onset of the heat-transfer crises associated with the drying out of the film, and we calculated the vapor content x_b corresponding to this power. At water flow rates up to 300 kg/h the determination of the boundary of transition to the dispersed flow was accomplished under isothermal conditions. Heat was not directed into the working section, since the power of the heater was sufficient to achieve the limit vapor content. Experiments involving heating in the working section yielded the same results with respect to the limit vapor content. At greater flow rates the boundary was always determined with a flow of heat both to the heater and to the working section. We also investigated the effect of the heated length of the section on the boundary of transition to dispersed flow. The measurement results are shown in Table 1. With a reduction in the length of the heated section this boundary, in accordance with the balance equation, shifts in the direction of lower gravimetric vapor contents

$$x_b = x_1 + \frac{\pi d \int_{l_1}^{l} q\,dl}{\gamma w F r},$$

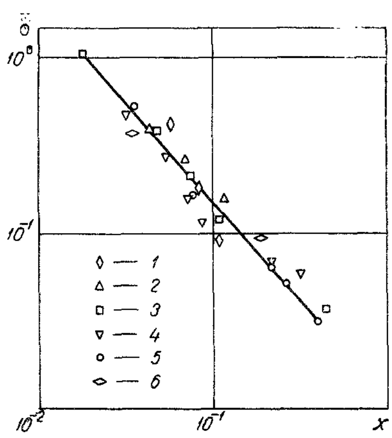

Fig. 3

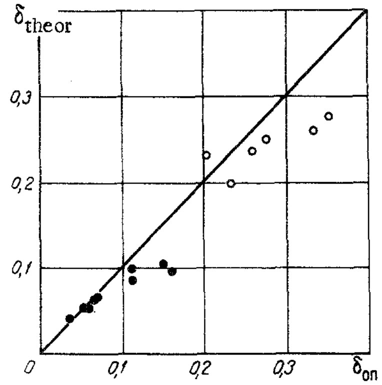

Fig. 4

Fig. 3. Average film thickness (mm) in the dispersed-annular flow of a vapor–water mixture in a tube with a diameter of 18 mm at a pressure of 1-2 atm abs as a function of the gravimetric vapor content: 1) G = 142 kg/h; 2) 200 kg/h; 3) 238 kg/h; 4) 300 kg/h; 5) 360 kg/h; 6) 375 kg/h.

Fig. 4. Comparison for experimental film thicknesses with the theoretical values for Re = 300.

where x_1 is the vapor content determining the onset of the dispersed-annular flow regime. The quantity x_1 is in good agreement with the Wallis formula [5], which has been tested in special experiments.

To measure the length of the hydrodynamic-stabilization segment in the dispersed-annular regime at various distances from the probe by means of which we measure the film thickness, we set up a turbulizer to stir the flow into a homogeneous mixture. The onset of stabilization was associated with the attainment of a constant film thickness. The dispersed-annular flow ahead of the turbulizer was designed to produce a mixture in the heater. All of the measurements were performed under adiabatic conditions. The results of these studies are shown in Fig. 1, from which it is evident that the length of the hydrodynamic-stabilization segment falls within the limits $(50\text{-}100)l/d$. The heat-transfer crises data and the data on the transfer of heat to two-phase mixtures, derived with tubes shorter than 100d, should be treated as the results for a hydrodynamically nonsteady film flow regime.

In particular, references [6-9] are devoted to a study of the hydrodynamic relationship in a system including the turbulent core of the gas and the liquid film at the tube wall, with the friction at the boundary of phase separation determining the velocity profile in the liquid phase.

The authors of [6-8] assumed a certain velocity profile in the film to determine its thickness, its flow rate, and the friction at the surface of phase separation.

Tippets [9] analyzed the flow stability in the film by the method of small perturbations for the potential flow. Idealized sinusoidal waves were examined at the separation boundary, while viscous friction was not taken into consideration. The liquid flow regime was assumed to be one of developed turbulence, whose characteristics are determined from Prandtl theory. Further development for the analytical method can be found in [10-13]. In most of the solutions the acceleration and the transfer of mass at the boundary of phase separation are neglected.

In the article by Levi [13] the expression for the determination of film thickness was derived with consideration of the pressure drop associated with acceleration and with consideration of mass transfer. The data of [20] are used for the determination of the function

$$F\left(\frac{\delta}{R}\right) = \sqrt{\frac{\tau}{(\rho' - \rho_c)\,\bar{w}_c(\bar{w}_c - \bar{w}_f)}} ,$$

associating the tangential stress at the boundary of the liquid film with the core of the film and the relative film thickness. The function $F(\delta/R)$ is found from the measured values of dp/dz and δ. The magnitude of

TABLE 2. Characteristics of the Dispersed-Annular Flow Regime Based on the Experimental Data for a Vapor–Water Mixture

Expt. No.	kg/m^2·sec	$q \cdot 10^{-6}$, kcal/m^2·h	x_1	x out	in(ws) kg/cm^2	$\frac{\Delta P}{dl} \cdot 10^4$, kg/cm^2·cm	δ, mm	φ
1	145,0	0,085	0,054	0,054	1,12	—	0,405	—
2	145,0	0,105	0,054	0,081	1,14	—	0,175	—
3	145,0	0,136	0,054	0,105	1,20	—	0,035	—
1	218,7	0,105	0,046	0,031	1,17	3,13	1,08	0,727
2	218,7	0,141	0,046	0,069	1,22	3,27	0,260	0,886
3	218,7	0,195	0,046	0,118	—	4,23	0,150	0,944
1	260,7	0,116	0,040	0,014	1,17	3,60	1,1	0,714
2	260,7	0,152	0,040	0,043	1,22	4,25	0,355	0,874
3	260,7	0,180	0,040	0.067	1,30	5,03	0,205	0,923
4	260,7	0,228	0,040	0,102	1,43	5,82	0,115	0,958
5	260,7	0,566	0,040	0,416	2,45	13,33	0,035	0,996
1	328,1	0,188	0,030	0,030	1,27	5,40	0,475	0,837
2	328,1	0,206	0,030	0,051	1,34	5,88	0,275	0,894
3	328,1	0,228	0,030	0,071	1,41	6,56	0,150	0,928
4	328,1	0,253	0,030	0,087	1,49	7,02	0,115	0,954
5	328,1	0,422	0,030	0,206	2,05	10,85	0,070	0,988
6	328,1	0,562	0,030	0,309	2,51	13,00	0,055	0,995
1	395,3	0,209	0,031	0,033	1,32	5,10	0,52	—
2	395,3	0,288	0,031	0,075	1,49	7,50	0,16	—
3	395,3	0,512	0,031	0,203	2,35	7,55	0,065	—
4	395,3	0,644	0,031	0,257	2,79	—	0,050	—
1	406,5	0,226	0,032	0,032	1,33	—	0,365	—
2	406,5	0,373	0,032	0,111	0,86	—	0,235	—
3	406,5	0,533	0,032	0,191	2,41	—	0,095	—

the slip, i.e., the ratio of the average gas and liquid velocities, for the case in which γ'/γ'' = 1-200, is approximated by the expression $s = \bar{w}''/\bar{w}' = (\gamma_1/\gamma'')^{1/3}$. The exponent (1/3) was chosen to achieve good agreement with the experimental data.

In [14] an analytical expression was also found for the film thickness as a function of the pressure gradient. References [15, 16] are devoted to the experimental study of problems associated with film thickness and pressure gradients in two-phase water–air systems. There are few simultaneous measurements of film thicknesses and pressure gradients [17, 18] for vapor–liquid systems.

When we measured the thicknesses of the liquid films at various flow rates for the mixture and at various vapor contents we used an electric probe mounted at the end of the working section, beyond the heating zone. The probe was designed to permit its displacement along the tube radius, with a controlled accuracy of 0.005 mm. Figure 2 shows the manner in which the probe was connected into the measuring circuit. Its basic elements include the sound-pulse generator which transmits ac pulses to the probe, the load resistance R_1, a frequency filter, an amplifier, an oscillograph, and a counter with a special unit making it possible to receive two forms of information.

When the capacitor C_2 is disconnected, the counter counts the number of pulses during the period in which the probe is in contact with the liquid. The ratio of this contact time $\tau_{1-\varphi}$ to the total counting time τ characterizes the true local content of liquid at the point of the probe. The ratio of the time τ_φ, when there is no contact with the liquid (the vapor phase), to the counting time will be approximately equal to the true vapor content φ of the mixture at that point.

When the capacitor C_2 is connected, the counter counts the number of contacts made by the probe with the film, thus giving some indication as to the wave structure of the film's surface layer. The circuit provides for the recording of the pulses on a loop oscillograph. For the average film thickness we assumed the distance between the probe and the wall at which the relative time of contact between the probe and the film amounted to 50%.

Figure 3 shows the film-thickness data as a function of the gravimetric weight content x for various mixture flow rates which, in logarithmic coordinates, are discharged by a single function. This apparently suggests that the effect of the over-all flow rate of the mixture manifests itself twice. On the one hand, at large liquid flow rates thicker films should develop at the inlet, given the same vapor content at the point of measurement; on the other hand, high velocities for the vapor phase, corresponding to large flow rates, results in more substantial entrainment of the liquid from the film to the core. It is probable that these two processes offset each other to some extent. We see from Fig. 3 that the average thickness of the liquid film is approximately inversely proportional to the vapor content.

The average vapor content in the cross section is found from the expression

$$\varphi_{av} = \frac{\int\limits_0^R \varphi r dr}{\int\limits_0^R r dr}. \tag{1}$$

The pressure gradient was measured at the middle of the working section. The pressure was sampled through two holes 600 mm apart. The pressure difference was transmitted to strain gauges whose electrical pulse was recorded on a loop oscillograph.

The experimental data on the measurement of film thickness, volumetric vapor content, and pressure gradients, derived through measurements in a tube with a diameter of 18 mm, are shown in Table 2.

The results from the measurements of the film thickness were compared with the theoretical data on the basis of the formulas proposed by Kirillov:

for laminar film flow

$$\frac{\delta}{R} = \frac{\psi(1-x)}{1-\psi(1-x)}\frac{\gamma''}{\gamma'} + 5.95\left(\frac{gR\mu'}{G}\right)^{0.375}\left(\frac{\mu'}{\mu''}\right)^{0.125}\left(\frac{\gamma''}{\gamma'}\right)^{0.5}\frac{\sqrt{\psi(1-x)}}{[1-\psi(1-x)]^{0.875}}, \tag{2}$$

for turbulent film flow

$$\frac{\delta}{R} = \frac{\psi(1-x)}{1-\psi(1-x)}\frac{\gamma''}{\gamma'} + 0.353\left[\frac{\psi(1-x)}{1-\psi(1-x)}\right]^{0.875}\left(\frac{\gamma''}{\gamma'}\right)^{0.375}\left(\frac{\nu'}{\nu''}\right)^{0.125}. \tag{3}$$

The calculations were performed in three variants:

1) in the assumption of laminar film flow and purely annular flow, i.e., in the absence of liquid entrainment to the core ($\psi = 1$);

2) in the assumption of laminar flow $\psi \neq 1$;

3) in the assumption of turbulent flow $\psi \neq 1$.

Consideration of entrainment was accomplished on the basis of the Chearer and Nedderman method [14], according to which the quantity ψ can be calculated from the experimental data on film thicknesses and pressure gradients. The authors of [14], on the basis of a number of simplifying assumptions and using the universal velocity profile in the film, proposed a graph for the calculation of the liquid flow rate in the film. The calculations for the annular model of the flow ($\psi = 1$) demonstrated the unsatisfactory agreement with experiment. The theoretical quantities for the thicknesses were approximately double those of the experimental data. Consideration of entrainment through use of the results from [14] conversely led to an understatement of the theoretical quantities.

Considering the entrainment of the liquid from the film in accordance with the method proposed in [19] causes the values of ψ taken from the graph in this paper to be overstated approximately by 25% in comparison with the experimental data [15]. Based on this correction factor, the calculated film thicknesses are in satisfactory agreement with our experimental data, and in the case of the greater thicknesses – corresponding to lower vapor contents and velocities – formula (3) yields better agreement for turbulent film, while in the case of smaller thicknesses formula (2) yields better agreement for laminar flow (Fig. 4). The tentative value for the critical Reynolds number is

$$\mathrm{Re}_{cr} = \frac{\bar{w}'\delta}{\nu} = 300 - 400.$$

NOTATION

x_b is the vapor content corresponding to the boundary of transition from the dispersed-annular to the dispersed flow regime;

x_1 is the vapor content corresponding to the boundary of transition from the plug-type to the dispersed-annular flow;

d, R, and l	are, respectively, the diameter, the radius, and the length of the working section of the tube;
F	is the cross-sectional area;
r	is the heat of vapor formation, and the instantaneous radius of the tube;
δ	is the film thickness;
τ	is the shear stress at the wall, and time;
ρ'	is the density of the liquid phase;
ρ_c	is the density of the dispersed core;
$\bar{w}_c$	is the average velocity in the flow core;
$\bar{w}_f$	is the average velocity in the film;
φ	is the true volumetric vapor content;
G_f	is the liquid flow rate in the film;
G	is the flow rate of the mixture;
G'	is the flow rate of the liquid phase;
$\psi = G_f/G'$	is the fraction of the liquid flow rate flowing in the film.

LITERATURE CITED

1. C. Raisson, Rapport TT N-62 (texte presente an Symposium dIspRA, de Juin, 1966).
2. N. A. Radovicich and R. Moissis, MIT Report No. 7-7673-22, June (1962).
3. A. E. Bergles, R. F. Lopina, and M. P. Fiori, Journal of Heat Transfer, 89, C, 1 (1967).
4. M. Silvestrie, in: Problems of Heat Transfer [Russian translation], Atomizdat (1967), p. 199.
5. G. B. Wallis, AEEW-R142 (1962).
6. A. E. Dukler and O. P. Berglin, Chem. Engng. Progress, 48, 11 (1952).
7. G. H. Anderson and B. G. Mantzouranis, Chem. Engng. Sci., 12, 1 (1960).
8. G. F. Hewitt, AERE-R 3680 (1961).
9. F. E. Tippets, Journal of Heat Transfer, 86, C, 1 (1964).
10. S. S. Kutateladze and M. A. Styrikovich, The Hydraulics of Gas–Liquid Systems [in Russian], GEI (1958).
11. P. A. Semenov, Zh. Tekh. Fiz., 20 (1950).
12. B. I. Konobeev et al., Dokl. Akad. Nauk SSSR, 117, 4 (1957).
13. S. Levi, Int. Journal Heat Mass Transfer, 9, 3 (1966).
14. C. S. Chearer and R. M. Nedderman, Chem. Engng. Sci., 20, 7 (1965).
15. L. E. Gill and G. F. Hewitt, AERE-3935 (1962).
16. G. F. Hewitt, R. D. King, and P. C. Lovegrove, AERE-R 3921 (1962).
17. G. F. Hewitt, H. A. Kearsey, P. M. C. Lacey, and D. I. Pulling, AERE-R 4374 (1963).
18. G. F. Hewitt, H. A. Kearsey, P. M. C. Lasey, and D. I. Pulling, AERE-R 4864 (1965).
19. T. Quanc and I. D. Huyghe, Sympos. Two-Phase Flow, Exeter, Devon, England, SC-201-212 (1965).
20. Adorni et al., CISE Report R 35 (1961); R-53 (1963); R-73 (1963).